JOURNAL OF APPLIED PHYSICS VOLUME 88, NUMBER 9 1 NOVEMBER 2000

Depolarization of evanescent waves scattered by laser-trapped gold particles: Effect of particle size

Min Gu[a)]
Centre for Micro-Photonics, School of Biophysical Sciences and Electrical Engineering, Swinburne University of Technology, P.O. Box 218, Hawthorn, Victoria 3122, Australia

Puchun Ke
School of Communications and Informatics, Victoria University, P.O. Box 14428, MCMC, Victoria 8001, Australia

(Received 8 May 2000; accepted for publication 14 August 2000)

Depolarization of evanescent waves scattered by laser-trapped gold particles of 0.1, 0.5 and 2 μm in diameter is experimentally characterized in order to reveal its dependence on the size of particles. It is found that the degree of polarization of scattered evanescent waves decreases with the size of gold particles, which is contrary to that previously observed for dielectric particles. This feature becomes advantageous in particle-trapped near-field microscopy since less depolarized photons carry more information of a sample. With the help of polarization gating, this property is demonstrated in images of the evanescent wave interference pattern as well as the surface of a glass prism. © *2000 American Institute of Physics.* [S0021-8979(00)05722-4]

I. INTRODUCTION

Scattering of a plane electromagnetic wave by a small particle, usually termed Mie scattering, has been extensively studied.[1–4] The scattered wave exhibits depolarization, which depends on the size of particles; the smaller the particle the stronger the depolarization. If a particle is scattered by an evanescent wave,[5–8] referred as to near-field Mie scattering, cross polarization components[5] can occur because of the spatially asymmetric distribution of an evanescent wave and multiple interaction between a particle and a boundary where the evanescent wave generates. It is important to have accurate knowledge regarding the dependence of depolarization on particle size in near-field Mie scattering as it determines image quality in near-field scanning optical microscopy (NSOM) employing a metallic tip[6,9] or a laser-trapped particle.[10–14]

Recently, depolarization of near-field Mie scattering has been characterized[12,13,15] including the use of a laser-trapped dielectric particle.[12,13] It has been shown that the degree of polarization of the scattered evanescent wave collected by a trapping objective increases with the size of dielectric particles.[13] It has also been demonstrated that employing polarization gating in particle-trapped NSOM leads to an improvement in image contrast of the evanescent wave interference fringes.[12] Although image quality of particle-trapped NSOM can be improved appreciably with a metallic particle, which results in strong scattering and surface plasmon resonance,[11] the effect of a trapped metallic particle on the degree of polarization and the dependence of the degree of polarization on particle size have not been addressed.

This article reports on a detailed experimental study of evanescent waves scattered by trapped gold particles of different sizes. In Sec. II, the degree of polarization of scattered evanescent waves by gold particles is measured to reveal its dependence on the size of particles. In Sec. III, polarization gating is applied to particle-trapped NSOM for image improvement in imaging the evanescent wave interference pattern and the surface of a glass prism. A final conclusion is given in Sec. IV.

II. DEPOLARIZATION OF EVANESCENT WAVES SCATTERED BY LASER-TRAPPED METALLIC PARTICLES

The experimental setup and procedure used in this article were the same as those described in Fig. 1 of Refs. 12 and 13. Gold particles of $\phi = 0.1$, 0.5, and 2 μm in diameter, suspended in water, were placed on the top surface of an SF10 prism with optical flatness $\lambda/10$, respectively. One gold particle was trapped by a high numerical aperture objective at the bottom of the particle, in which case the trapped particle was always in touch with the prism surface.[11]

The strength of the evanescent wave scattered by a trapped gold particle η was measured and is displayed in Fig. 1 for gold particles of $\phi=0.1$ μm (a), 0.5 μm (b), and 2 μm (c) for the incident angle from $\theta=56°$ to 62° of the He–Ne laser beam. I_s and I_p were measured for *s*- and *p*-polarized illumination beams without an analyzer, I_{ss} and I_{sp} were measured with an analyzer of the polarization direction parallel and perpendicular to the incident *s*-polarized He–Ne beam, respectively, and I_{pp} and I_{ps} were measured with an analyzer parallel and perpendicular to the incident *p*-polarized He–Ne beam, respectively. It can be seen from Fig. 1 that the signal strength of the scattered evanescent wave decreases with the incident angle of the He–Ne laser beam, which is similar to the behavior for dielectric particles.[13] This feature is understandable because the decay length of an evanescent wave above the surface of a prism is

---

[a)] Author to whom correspondence should be addressed; electronic mail: mgu@swin.edu.au

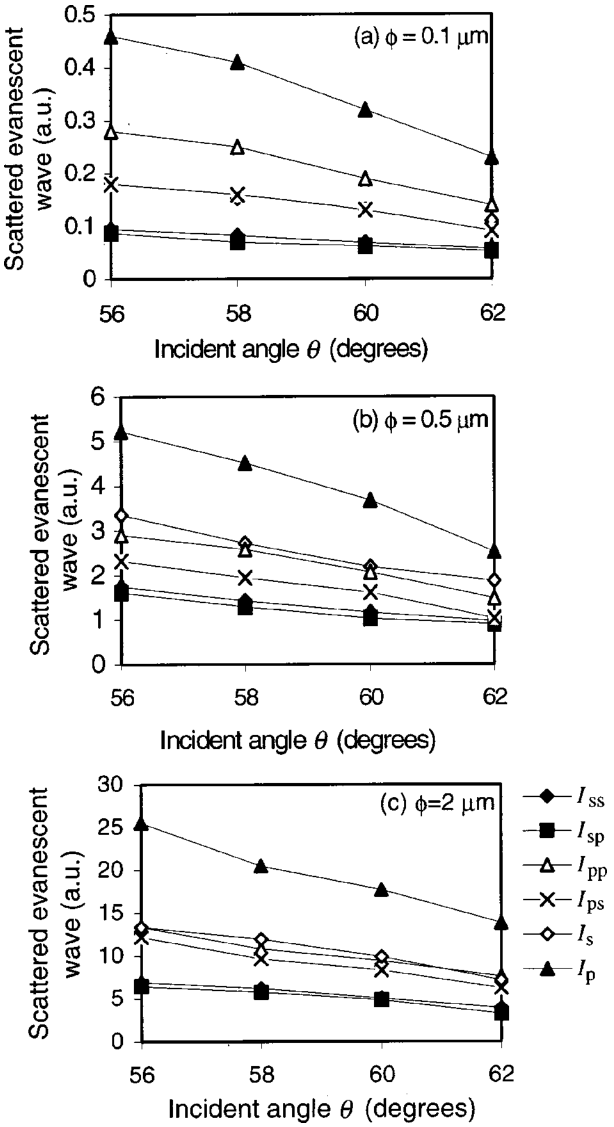

FIG. 1. Dependence of the signal strength of scattered evanescent waves on the incident angle θ of the He–Ne laser beam for gold particles: (a) $\phi=0.1$ μm; (b) $\phi=0.5$ μm; (c) $\phi=2$ μm.

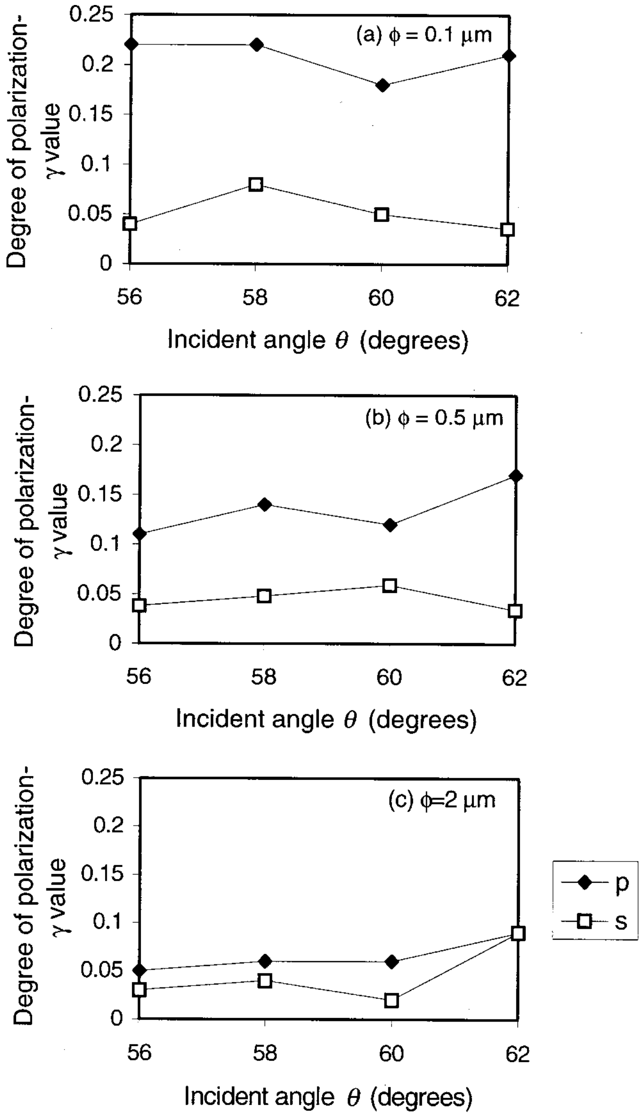

FIG. 2. Dependence of the degree of polarization of scattered evanescent waves on the incident angle θ of the He–Ne laser beam for gold particles: (a) $\phi=0.1$ μm; (b) $\phi=0.5$ μm; (c) $\phi=2$ μm.

decreased as the incident angle of the illumination He–Ne laser is increased. As a result, the interaction between the particle and the evanescent field becomes weak. Further, the signal strength of the scattered evanescent wave increases with the size of a particle for a given angle of incidence, as expected from the previous experiment.[11] The dependence of the averaged signal strength on the size of particles reveals an approximate linear relation given by $\eta \cong 10.6\phi - 1.3$.

It is also seen from Fig. 1 that for both *s*- and *p*-polarized illumination beams, cross-polarization components appear in the scattered signals, indicating the occurrence of depolarization in the scattering of evanescent waves by laser-trapped gold particles. This depolarization process can be quantified by the degree of polarization, γ, defined as

$$\gamma = \frac{I_{\parallel} - I_{\perp}}{I_{\parallel} + I_{\perp}}, \tag{1}$$

where subscripts $\parallel$ and $\perp$ denote the analyzer direction parallel or perpendicular to the plane of incidence of the He–Ne laser beam, respectively.

The degree of polarization γ for the three types of gold particles is illustrated in Fig. 2. It is clearly seen that the scattering between a gold particle and an evanescent wave is dependent on the incident angle as well as on the polarization state of the illumination He–Ne laser beam. To confirm our results, the degree of polarization of scattered evanescent waves was measured as a function of the polarization angle i of the He–Ne laser beam with respect to its plane of incidence. Figures 3(a), 3(b), and 3(c) correspond to gold particles of $\phi=0.1$ μm, 0.5 μm, and 2 μm at $\theta=62°$, respectively. Similar to the situation for dielectric particles,[12] a ''v'' shaped pattern of the degree of polarization appears in each case when the polarization angle i is altered from 0° to 90°. As expected, depolarization becomes the strongest near $i=45°$.

The dependence of the degree of polarization of the scattered evanescent wave on the size of particles is summarized

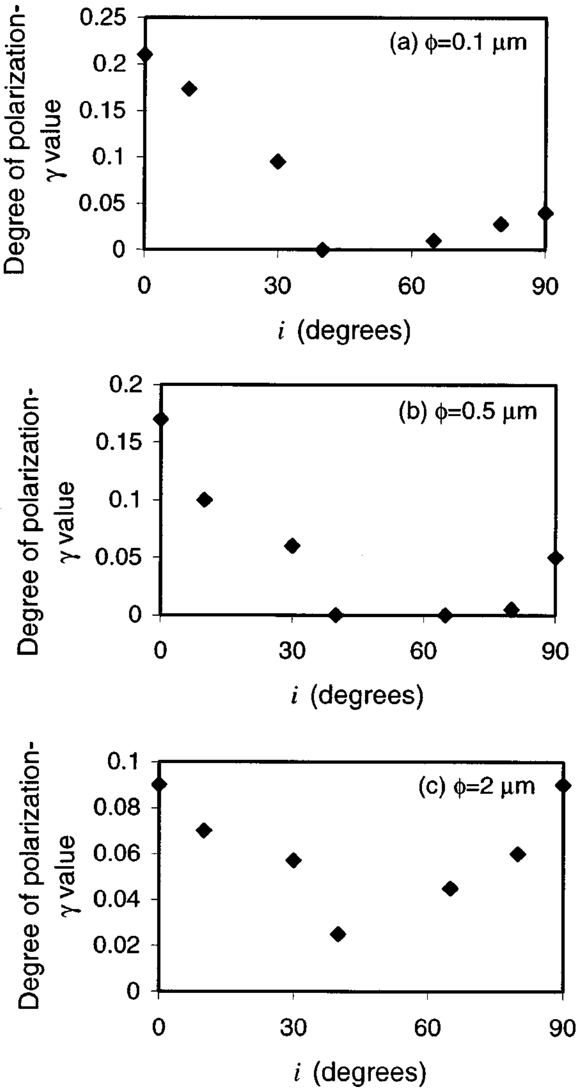

FIG. 3. Degree of polarization of scattered evanescent waves as a function of the polarization direction *i* of the He–Ne laser beam relative to the plane of incidence for gold particles at $\theta=62°$: (a) $\phi=0.1$ μm; (b) $\phi=0.5$ μm, (c) $\phi=2$ μm.

in Fig. 4. Here $p1$, $p2$, $p3$, and $p4$ represent the results measured for *p*-polarized He–Ne beam illumination at incident angles of $\theta=56°$, 58°, 60°, and 62°, respectively, while $s1$, $s2$, $s3$, and $s4$ correspond to those for *s*-polarized beam illumination at the corresponding incident angles. Figure 4 clearly shows that the degree of polarization of the scattered evanescent wave decreases with the size of gold particles particularly for *p*-polarized illumination. For an *s*-polarized illumination beam, the averaged degree of polarization is $\gamma=0.052$, 0.04, and 0.028 for $\phi=0.1$, 0.5, and 2 μm, respectively, while for a *p*-polarized illumination beam, the averaged degree of polarization is $\gamma=0.208$, 0.135, and 0.065 for $\phi=0.1$, 0.5, and 2 μm, respectively. This result differs from that observed for dielectric particles in which case the degree of polarization increases monotonically with the size of dielectric particles.[13]

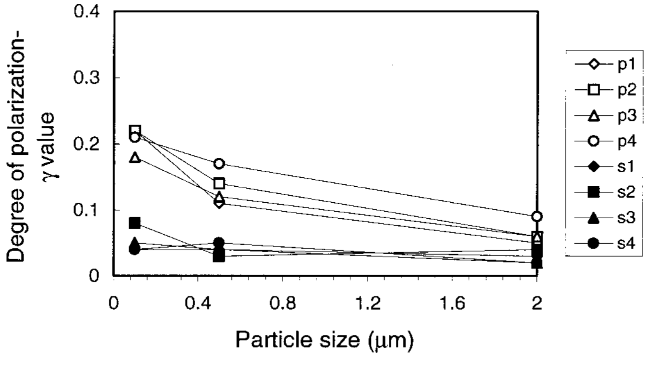

FIG. 4. Degree of polarization as a function as the size of gold particles under *s*- and *p*-polarized beam illumination.

This difference may be related to the generation of surface plasmon resonance.[3,16,17] For a metallic particle illuminated with an evanescent wave, the scattered field may be enhanced due to the generation of surface charges. The surface charges form an oscillating distribution under the illumination of evanescent waves and show the characteristics of surface plasmon, which leads to the enhanced scattering for both *p*- and *s*-polarized illumination. However, for *p*-polarized illumination, the enhancement of surface plasmon resonance may occur[3] and becomes stronger for a smaller particle.[17] These physical processes may lead to the feature for gold particles observed in Fig. 4 and can be analyzed according to the radiation pattern of dipoles caused by surface charges[18] or the multiple multipole method.[7,8,19] But this theoretical study is beyond the scope of this article.

III. IMAGING OF PARTICLE-TRAPPED NSOM BY POLARIZATION GATING

In this section, with the aid of polarization gating which is based on the principle that less depolarized photons carry more information of a sample,[12,13] we examine the impact of depolarization of evanescent waves scattered by trapped gold particles on particle-trapped NSOM. Using the same approach as described in Refs. 12 and 13, we obtained images of evanescent wave interference pattern with I_s, I_{ss}, I_{sp}, I_p, I_{pp}, and I_{ps}. Figures 5, 6, and 7 give typical images and the corresponding intensity cross sections with laser-trapped gold particles of $\phi=0.1$, 0.5, and 2 μm, respectively. The scanning speed for imaging was maintained at 1.5 μm/s in the *x* and *y* directions for three types of gold particles.

According to the intensity cross sections, the averaged value of image contrast can be defined as

$$c=\frac{I_{\max}-I_{\min}}{I_{\max}+I_{\min}}, \tag{2}$$

where $I_{\max}$ and $I_{\min}$ are the maximum and minimum intensity of the cross sections. The value of the contrast *c* for Figs. 5–7 is summarized in Table I. As expected, the image contrast derived with I_{pp} is the best for a given size of particles. The improvement in image contrast with I_{pp} is more pronounced than that with I_{ss} except for $\phi=0.1$ μm. This result is caused by the fact that the degree of polarization for $\phi=0.1$ μm under *s*-polarized illumination is much smaller than that under *p*-polarized illumination. As a result, the use of polarization gating in the former case can lead to a pronounced effect on image improvement. For a given sensitiv-

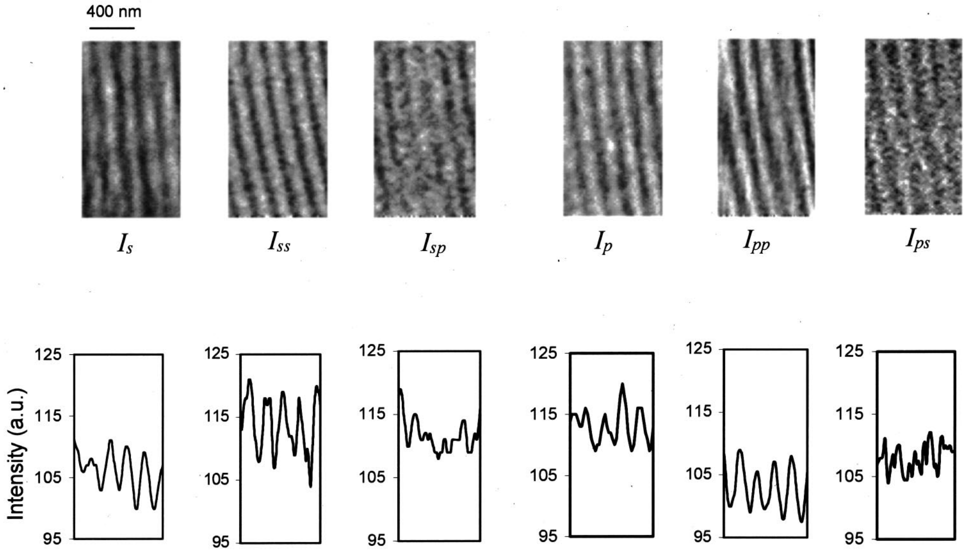

FIG. 5. Images (top) and the intensity cross sections (bottom) of evanescent wave interference patterns for different polarization directions of a polarizer and an analyzer for $\phi=0.1$ μm.

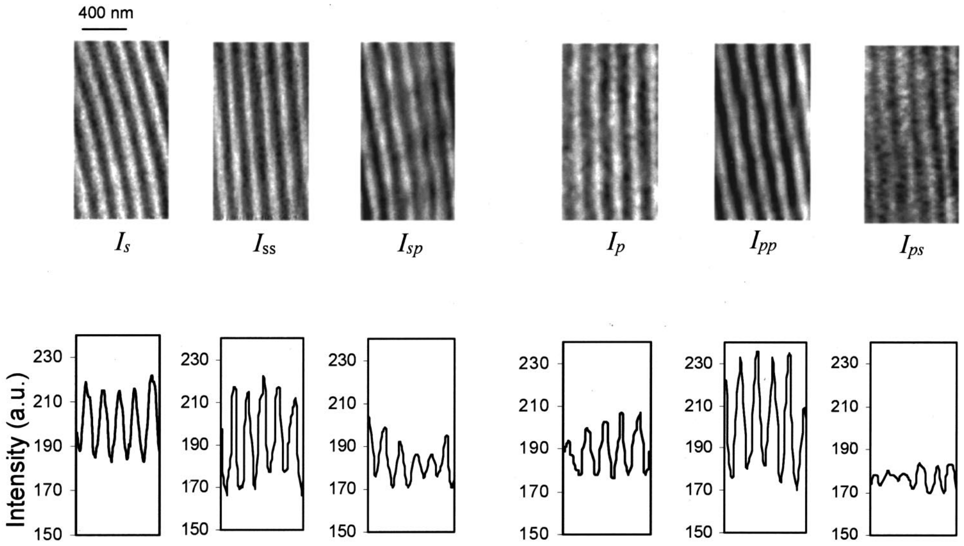

FIG. 6. Images (top) and the intensity cross sections (bottom) of evanescent wave interference patterns for different polarization directions of a polarizer and an analyzer for $\phi=0.5$ μm.

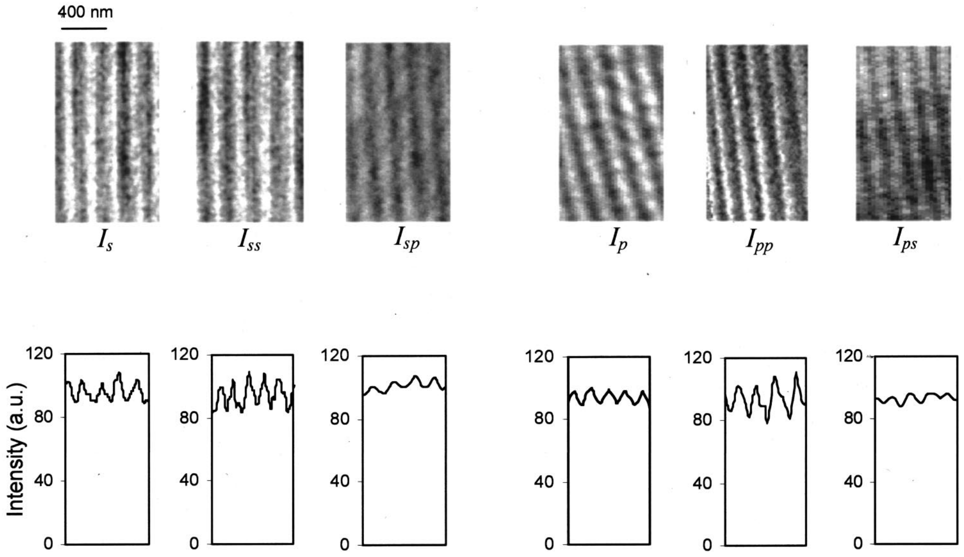

FIG. 7. Images (top) and the intensity cross sections (bottom) of evanescent wave interference patterns for different polarization directions of a polarizer and an analyzer for $\phi=2$ μm.

TABLE I. Image contrast of evanescent wave interference patterns obtained by trapped gold particles of diameter 0.1, 0.5, and 2 μm, respectively.

Particle diameter (μm)	I_s[a]	I_{ss}[b]	I_{sp}[b]	I_p[a]	I_{pp}[c]	I_{ps}[c]
2	7%	10%	4%	6%	11%	3%
0.5	9%	12%	5%	7%	13%	3%
0.1	3%	6%	2%	4%	7%	2%

[a] I_s and I_p: scattered signal without using an analyzer under *s* and *p* polarized beam illumination.

[b] I_{ss} and I_{sp}: scattered signal with *s* and *p* analyzers under *s*-polarized beam illumination.

[c] I_{ps} and I_{pp}: scattered signal with *s* and *p* analyzers under *p* polarized beam illumination.

ity in detection, the amount of improvement in image contrast depends on signal strength and noise level. Consequently, the image contrast for $\phi = 0.5$ μm is the optimum under our experimental condition, which is similar to the case for dielectric particles.[13]

The use of polarization gating for improving image contrast in NSOM with a trapped gold particle was also conducted for the surface of a BK7 prism with optical flatness $\lambda/4$. The polarizer was fixed at a *p*-polarized state and the polarization direction of the analyzer was altered from the parallel direction to the perpendicular direction with respect to that of the polarizer. Images of the surface of the BK7 prism are shown in Fig. 8 for a gold particle of $\phi = 0.1$ μm. Compared with the image recorded without an analyzer [Fig. 8 (a)], the image contrast for an analyzer of the polarization direction parallel to that of the polarizer [Fig. 8 (b)] is obviously sharper. By contrast, the image is degraded when the polarization direction of the analyzer is perpendicular to that of the polarizer, as shown in Fig. 8(c). This result is consistent with Fig. 5, showing that signal strength and depolarization caused by scattering of evanescent waves are crucial for image formation and that polarization gating is effective for image enhancement.

As a comparison, Fig. 9 gives images of the surface of the prism with a trapped dielectric particle under the same polarization gating condition as in Fig. 8. In addition to the demonstration of the advantage of polarization gating, Fig. 9 also demonstrates that imaging with a laser-trapped gold particle is advantageous over a dielectric particle in that better image contrast can be obtained in the former case. This result agrees with that reported previously.[11]

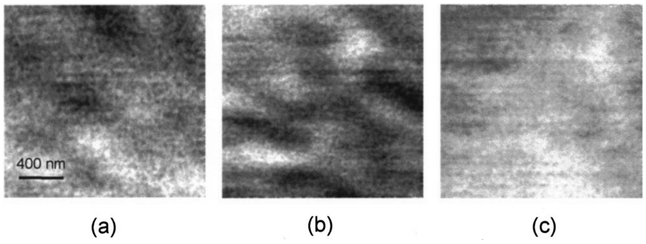

FIG. 8. Images of the surface of a BK7 prism with a gold particle of 0.1 μm in diameter: (a) no analyzer; (b) the polarization direction of the analyzer is parallel to that of the polarizer; (c) the polarization direction of the analyzer is perpendicular to that of the polarizer.

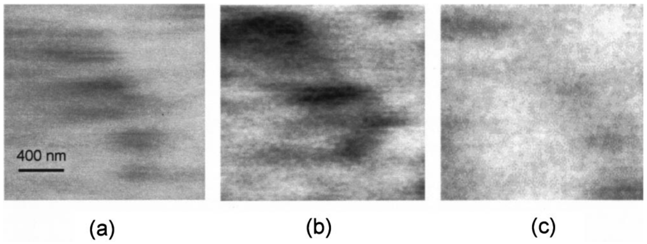

FIG. 9. Images of the surface of a BK7 prism with a polystyrene particle of 0.1 μm in diameter: (a) no analyzer; (b) the polarization direction of the analyzer is parallel to that of the polarizer; and (c) the polarization direction of the analyzer is perpendicular to that of the polarizer.

IV. CONCLUSION

The degree of polarization of the scattered evanescent wave by a trapped gold particle decreases with the size of particles, in particular, under *p*-polarized beam illumination. This polarization-dependent feature is possibly related to the enhancement of surface plasmon resonance associated with small metallic particles. The effect of depolarization on image quality in particle-trapped NSOM has been examined in terms of polarization gating. For example, in the case of a gold particle of $\phi = 0.1$ μm, the enhancement factor of image contrast of the evanescent wave interference pattern is 2 and 1.75 under *s*- and *p*-polarized beam illumination, respectively. Such image enhancement has also been observed in imaging the surface structure of a prism. These results confirm that less depolarized photons of the scattered evanescent wave carry more information of an object. In this sense, the use of a gold particle of small size may prove advantageous because the scattered evanescent wave is less depolarized.

ACKNOWLEDGMENTS

The authors thank the Australian Research Council for its support. P. K. was supported by the Australian Postgraduate Award Scholarship. The experimental work presented in this article was conducted at Victoria University and part of the manuscript was completed when M. Gu visited Osaka University with support from the Japan Society for the Promotion of Science.

[1] M. Born and E. Wolf, *Principles of Optics* (Pergaman, New York, 1980).
[2] P. W. Barber and R. K. Chang, *Optical Effects Associated with Small Particles* (World Scientific, Singapore, 1988).
[3] M. Kerker, *The Scattering of Light and Other Electromagnetic Radiation* (Academic, New York, 1969).
[4] C. F. Bohern and D. R. Huffman, *Absorption and Scattering of Light by Small Particles* (Wiley, New York, 1983).
[5] H. Chew, D. S. Wang, and M. Kerker, Appl. Opt. **18**, 2679 (1979).
[6] M. Lester and M. Nieto-Vesperinas, Opt. Lett. **24**, 936 (1999).
[7] R. Wannemacher, A. Pack, and M. Quinten, Appl. Phys. B: Lasers Opt. **68**, 225 (1999).
[8] M. Quinten, a. Pack, and R. Wannemacher, Appl. Phys. B: Lasers Opt. **68**, 87 (1999).
[9] Y. Inouye and S. Kawata, Opt. Lett. **19**, 159 (1994).
[10] S. Kawata, Y. Inouye, and T. Sugiura, Jpn. J. Appl. Phys., Part 2 **33**, L1725 (1994).
[11] M. Gu and P. Ke, Opt. Lett. **24**, 74 (1999).
[12] M. Gu and P. Ke, Appl. Phys. Lett. **75**, 175 (1999).
[13] P. Ke and M. Gu, Opt. Commun. **171**, 205 (1999).
[14] L. Malmqvist and M. Mertz, Opt. Lett. **19**, 853 (1994).

[15] D. Prieve and J. Walz, Appl. Opt. **32**, 1629 (1993).
[16] L. Novotny, E. J. Sánchez, and X. S. Xie, Ultramicroscopy **71**, 21 (1998).
[17] B. J. Messinger, K. U. von Raben, R. K. Chang, and P. W. Barber, Phys. Rev. B **24**, 649 (1981).
[18] D. J. Griffiths, *Introduction to Electrodynamics* (Prentice-Hall, London, 1981).
[19] Peter Török, P. Higdon, R. Juskaitis, and T. Wilson, Opt. Commun. **155**, 335 (1998).